Research paper

Popping of g-C$_3$N$_4$ mixed with cupric nitrate: Facile synthesis of Cu-based catalyst for construction of C−N bond

Shaoyu Yuan [a], Penglei Cui [b], Yunrui Zhang [a], Hong Zhang [a,*], Li Huo [a], Yongjun Gao [a,*]

[a] College of Chemistry and Environmental Science, Hebei University, Baoding 071002, China
[b] College of Science, Agricultural University of Hebei, Baoding 071001, China

Abstract

A novel strategy to synthesize copper-based nanoparticles supported on carbon nitride (C$_3$N$_4$) was developed by popping of mixture containing C$_3$N$_4$ and cupric nitrate. Characterizations such as X-ray photoelectron spectroscopy (XPS) and X-ray diffraction (XRD) indicate that the structure of g-C$_3$N$_4$ maintained although a popping process occurred. High resolution transmission electronic microscopy (HRTEM) characterization illustrated that copper-based nanoparticles with diameter of < 1 nm were well distributed on g-C$_3$N$_4$. This kind of copper catalyst exhibits high catalytic activity and selectivity in arylation of pyrazole, a simple and effect strategy to construct C−N bond in organic chemistry. According to the results of control experiments and characterizations, cuprous oxide should be the catalytic active phase in the supported coper-based catalyst.

© 2018, Institute of Process Engineering, Chinese Academy of Sciences. Publishing services by Elsevier B.V. on behalf of KeAi Communications Co., Ltd. This is an open access article under the CC BY-NC-ND license (http://creativecommons.org/licenses/by-nc-nd/4.0/).

Keywords: C−N coupling; N-arylation; Carbon nitride; Catalysis; Copper-based catalyst
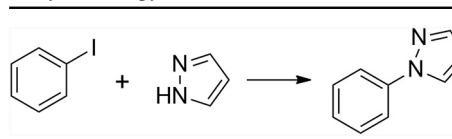
1. Introduction

Copper (Cu), a 3d transition metal element with valence electron structure of $3d^{10}4s^1$, possesses wide range of accessible oxidation states such as Cu^0, Cu^I, Cu^{II} and even Cu^{III} [1,2]. This property endows Cu-based catalyst with ability to promote and undergo various reactions [2]. Cu-based salts and complexes exhibits excellent catalytic performance as a potential substitute for noble metal catalysts in some traditional organic reactions such as the constructions of C−C bond and C−N bond [3–7]. However, the drawbacks of homogeneous catalytic systems hamper the developments and applications of Cu-based homogeneous catalysts especially in synthesis of drugs. Consequently, Cu-based nanocatalysts with advantages of heterogeneous catalytic system, such as Cu, CuO or Cu$_2$O nanoparticles, attract more and more attentions from academic and industrial researchers in recent years [2,8−10]. In general, the synthesis of free-standing Cu-based nanoparticles usually need surfactants which maybe impact the catalytic performance by hampering substrates to interact with active sites [11−14]. So, inorganic compounds, such as metal oxide, carbon materials, SiO$_2$, etc. are used to support Cu-based nanoparticles during the synthesis [15−18]. Appropriate support not only facilitate the distribution of nanoparticles but also improve the catalytic activity of active components. A variety of strategies are developed to synthesize supported Cu-based nanocatalysts with excellent catalytic performance in some organic reactions. To achieved Cu-based nanoparticles with uniform size and fine distribution on support, conditions in synthesis should be carefully screened and controlled. It will be significant supplement for Cu-based catalysis to develop supported Cu-based nanoparticles for traditional organic reaction (Tables 1 and 2).

Table 1
N-arylation of pyrazole with iodobenzene under different conditions.[a]
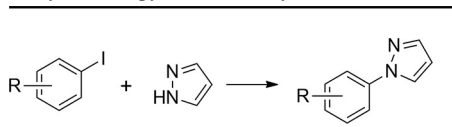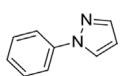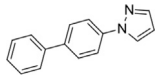
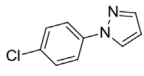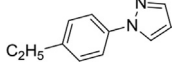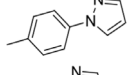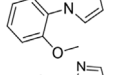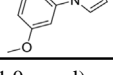| Entry	Catalyst	Base	Yield/%
1	blank	Cs_2CO_3	0
2	n-Cu-g-C_3N_4	Cs_2CO_3	91.3
3	g-C_3N_4	Cs_2CO_3	0
4	$Cu(NO_3)_2$	Cs_2CO_3	0
5	c-Cu-g-C_3N_4	Cs_2CO_3	11.4
6	s-Cu-g-C_3N_4	Cs_2CO_3	26.5
7[b]	n-Cu-g-C_3N_4	Cs_2CO_3	100
8	n-Cu-g-C_3N_4	NaOH	42.4
9	n-Cu-g-C_3N_4	KOH	69.1
10	n-Cu-g-C_3N_4	Na_2CO_3	4.7
11	n-Cu-g-C_3N_4	K_2CO_3	0

[a] Reaction conditions: aryl iodide (1.0 mmol), pyrazole (0.8 mmol), catalyst (0.01 g, 4 mol% Cu), acetonitrile (2 mL) and Cs_2CO_3 (1 mmol) 140 °C, 5 h.
[b] Reaction time is 12 h.

Table 2
N-arylation of pyrazole with aryl iodides.[a]

Entry	R	products	Yield/%
1	H		100
2	4-C_6H_5		93.6
3	4-Cl		100
4	4-C_2H_5		85.4
5	4-CH_3		59.8
6	2-CH_3O		80.0
7	3-CH_3O		100

[a] Reaction conditions: aryl iodide (1.0 mmol), pyrazole (0.8 mmol), catalyst (0.01 g, 4 mol% Cu), acetonitrile (2 mL) and Cs_2CO_3 (1 mmol) 140 °C, 12 h.

Graphitic carbon nitride (g-C_3N_4) has become a brilliant star in the field of material due to its special application in photocatalysis and other heterogeneous catalysis in recent years [19–22]. Cu-based nanocatalyst supported on g-C_3N_4 has been developed and applied in photocatalysis and some organic transformation [23–25]. The preparation of Cu-based nanocatalyst supported on g-C_3N_4 usually involves hydrothermal process, chemical reduction or thermal decomposition [24,26]. Therefore, the development of more simpler method

to fabricate Cu-based nanocatalyst supported on g-C_3N_4 is helpful to the field of Cu-based catalysis. In our research, an interesting phenomenon involving popping process of g-C_3N_4 modified by cupric nitrate was observed and applied to synthesize Cu-based nanocatalyst supported on g-C_3N_4. In addition, because N-arylation of heterocycles is an efficient approach to construct C—N bond, by which chemicals having substantial applications in pharmaceuticals, agricultural chemicals and polymers can be achieved [27–29], we evaluated the catalytic activity of our Cu-g-C_3N_4 catalysts in this kind of reactions. Excellent catalytic activity and selectivity were achieved in construction C—N bond through N-arylation of pyrazole. Control experiments indicated that popping process is a key factor for the fine distribution of Cu nanoparticles on g-C_3N_4.

2. Material and methods

2.1. Chemicals

Urea (AR, 99%) was produced by Shenyang chemical reagent factory. Cupric nitrate (AR, 99%) was purchased from Sinopharm Chemical Reagent Co. Ltd. Pyrazole (AR, 99%) and cesium carbonate (AR, 97%) were purchased from Shanghai Macklin Biochemical Co. Ltd. Iodobenzene (AR, 98%),1-iodo-4-methylbenzene (AR, 99%) and 4-Iodobiphenyl (AR, 97%) Aryl iodides were all purchased from Aladdln Industrlal Corporation. 4-Iodoanisole (AR, 98%) was purchased from Sain chemical technology (Shanghai) co. LTD. 1-iodo-3-methoxybenzene (AR, 98%), 1-Chloro-4-iodobenzene (AR, 99%) and 1-ehyl-4-iodobenzene (AR, 98%) were purchased from Alfa Aesar chemical co. LTD. Acetonitrile (AR, 99.5%) was purchased from Tianjin kemio chemical reagent co. Ltd. All chemicals are used directly without further treatment.

2.2. Preparation of g-C_3N_4

g-C_3N_4 was synthesized according to the reported method. In a typical process, urea (10.0 g) was calcined in covered crucible at 500 °C for 2 h in muffle furnace and then the light yellow g-C_3N_4 was achieved.

2.3. Preparation of Cu-g-C_3N_4

$Cu(NO_3)_2$ (0.3775 g) and g-C_3N_4 (0.5 g) were mixed and extensively milled in an agate mortar. Then the mixture powder was filled into a quartz tube and heated in a tubular furnace under nitrogen atmosphere (30 mL min^{-1}). At about 200 °C, the mixture was rapidly pyrolyzed and the light gray powder was achieved. Then the powder was collected into the quartz tube and continue heated to 400 °C under hydrogen atmosphere for 1 h. The product was achieved and label as n-Cu-g-C_3N_4. As control experiments, $CuCl_2$ and $CuSO_4$ were used as precursor to substitute $Cu(NO_3)_2$ and no rapid pyrolysis occurred during the heating process. The corresponding products were termed as c-Cu-g-C_3N_4 and s-Cu-g-C_3N_4.

2.4. Catalyst characterization

X-ray diffractometer (Bruker/Switzerland, D8 ADVANCE) with Cu kα ($\lambda = 1.5418$ Å) was used to record XRD patterns at 40 kV and 20 mA. The scanning electronic microscopy (SEM) analysis was conducted on a JSM-7500 microscopy (JEOL LTD./JAPAN, JSM-7500). The transmission electronic microscopy characterization was performed on a Tecnai G2 F20 instrument (FEI/USA, Tecnai G2 F20). X-ray photoelectron spectroscopy (XPS) was recorded on an AXIS-Ultra instrument using monochromatic Al Kα radiation (Kratos Analytical Ltd./JAPAN, AXIS-Ultra). Fourier Transform infrared spectrometer (Bruker/Germany, ALPHA) was used to conduct FTIR characterization. The content of copper in sample was determined by an inductively coupled plasma optical emission spectrometer (ICP-OES, Agilent 725 ICP-OES/USA) after the sample was processed in nitric acid.

2.5. Catalytic reaction

The N-arylation of pyrazole was carried out in a thick-wall glass vessel sealed with a Teflon lid (Beijing Synthware glass). Typically, aryl iodide (1.0 mmol), pyrazole (0.8 mmol), catalyst (0.01 g), acetonitrile (2 mL) and Cs_2CO_3 (1 mmol) were added in turn into the glass vessel. Then the glass vessel was sealed by the Teflon lid and heated on a metal heating mould at 140 °C. After reaction, n-dodecane (50 uL) was added into the mixture as internal standard. The mixture was diluted with ethyl acetate (10 mL) and vibrated extensively on a vortex mixer. The catalyst was filtered out and the filtrate was analyzed by gas chromatograph (GC, Agilent 6820A) with a HP-5 capillary column. The structure of the product was further determined by Gas chromatography−mass spectrometry (Agilent 7890B-5977 A GC/MSD).

3. Results and discussions

3.1. Synthesis and characterizations

It has been well known that nitrates could be used to prepare explosives due to their physicochemical properties [30].

If this property could be sensibly used in the preparation of supported catalysts, it would be a novel strategy to synthesize supported metal catalyst with high dispersion. As the popping process of graphene oxide reported in our previous report, it was helpful to well distribute metal component on graphene sheets [31]. When cupric nitrate was extensively mixed with g-C_3N_4 and then heated, it was found that the mixture could be exploded into fine powder at about 200 °C. Then the fine powder was continually heated to 400 °C under hydrogen atmosphere for 2 h and copper catalyst supported on g-C_3N_4, that is n-Cu-g-C_3N_4, could be achieved. When cupric nitrate was substituted by $CuCl_2$ or $CuSO_4$, no explosive occurred during the heating process and the products were named as c-Cu-g-C_3N_4 and s-Cu-g-C_3N_4. According to the measurement results of ICP-OES, the contents of copper in samples of n-Cu-g-C_3N_4, c-Cu-g-C_3N_4 and s-Cu-g-C_3N_4 were 21.1 wt%, 16.7 wt% and 19.3 wt%, respectively.

To determine the phase of copper components in the three copper-containing samples, XRD characterization was conducted firstly and the results are presented in Fig. 1a. XRD pattern of g-C_3N_4 exhibits two characteristic diffraction peaks locating at 2 θ = 12.9° and 27.3°, which point to the diffraction of (100) and (002) facets corresponding to the interplanar separation and interlayer stacking of aromatic systems of g-C_3N_4 [32]. After copper component were introduced and processed at 400 °C in hydrogen atmosphere, diffraction peak of (100) facet disappeared and (002) facet became broad, indicating the weakened periodic structure and decreased crystallinity of g-C_3N_4. For sample s-Cu-g-C_3N_4, obvious diffraction peaks corresponding to metal copper (Cu) and cuprous oxide (Cu_2O) appear, suggesting that there are two kinds of copper components in s-Cu-g-C_3N_4 and metal copper is dominant one. However, there is no obvious diffraction peaks pointing to copper components in the patterns of c-Cu-g-C_3N_4 and n-Cu-g-C_3N_4, which maybe results from the high dispersion, ultra-small size and low crystallinity of copper species.

To further investigate the molecular structure of g-C_3N_4, n-Cu-g-C_3N_4, c-Cu-g-C_3N_4 and s-Cu-g-C_3N_4, FTIR measurement were performed (Fig. 1b). The spectra of g-C_3N_4 exhibits
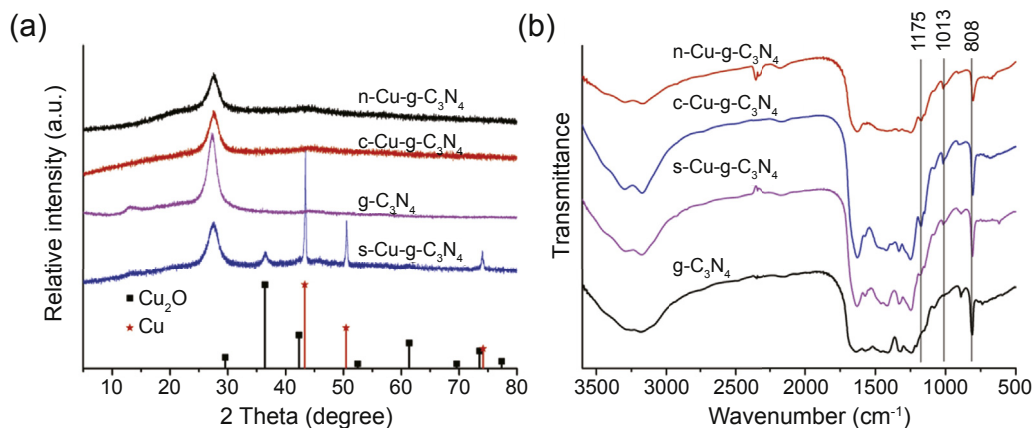
Fig. 1. (a) XRD patterns of g-C_3N_4, n-Cu-g-C_3N_4, c-Cu-g-C_3N_4 and s-Cu-g-C_3N_4, (b) FTIR spectra of g-C_3N_4, n-Cu-g-C_3N_4, c-Cu-g-C_3N_4 and s-Cu-g-C_3N_4.

the characteristic peaks at 808 cm^{-1}, 1200−1600 cm^{-1}, 3000−3500 cm^{-1}, corresponding to the s-triazine ring, C=N heterocycles and stretching vibration for N−H, respectively [33,34]. Although n-Cu-g-C_3N_4, c-Cu-g-C_3N_4 and s-Cu-g-C_3N_4 also have the three groups of characteristic peaks, the location and contour of these peaks slightly changed. For instance, the red shift of peak at 808 cm^{-1} occured in the three copper-containing samples. In addition, for n-Cu-g-C_3N_4, the fine peaks in the range of 1200−1600 cm^{-1} disappeared and became into one broad peak. All these results could be ascribed to strong interaction between copper with g-C_3N_4 in the sample n-Cu-g-C_3N_4 [35]. Besides, two new peaks at 1013 and 1175 cm^{-1} in the spectra of n-Cu-g-C_3N_4, c-Cu-g-C_3N_4 and s-Cu-g-C_3N_4, pointing to C−O−C and C−O vibration, could be clearly observed [32]. This result indicated that the oxygen-containing groups were introduced into g-C_3N_4 when copper components were introduced.

Then, the morphology of n-Cu-g-C_3N_4 was firstly characterized by HRTEM and well-distributed nanoparticles with diameter of < 1 nm supported on carbon-like structure could be differentiated if we carefully observe the HRTEM images (Fig. 2a and Fig. S1). So, elemental mapping analysis was further to confirm the well-distribution of copper element on g-C_3N_4, which clearly indicates that copper, carbon, nitrogen and oxygen elements are evenly distributed on n-Cu-g-C_3N_4 (Fig. 2b). For comparison, c-Cu-g-C_3N_4 and s-Cu-g-C_3N_4, with $CuCl_2$ and $CuSO_4$ as copper precursor respectively, were also characterized by HRTEM and the images are similar to the one of n-Cu-g-C_3N_4. No obvious nanoparticles supported on g-C_3N_4 could be clearly observed in the HRTEM images presented in Figs. S2 and S3. However, according to the XRD pattern of s-Cu-g-C_3N_4, large copper (oxide) nanoparticles should be existed in the sample. So, TEM images under different magnifications were screened. And some dark fields could be observed, which may be aggregated copper (oxide) components. In all, this result suggests that g-C_3N_4 is a suitable support to load and distribute copper-based components (Cu, Cu_2O or CuO) under our experimental conditions, which maybe resulted from the strong coordination of the uniformly distributed nitrogen atoms.

The chemical states of the different elements in n-Cu-g-C_3N_4 were analyzed by the X-ray photoelectron spectroscopy (XPS) and the results were shown in the Fig. 3. The C, N and O elements were obviously detected in the full XPS spectrum of g-C_3N_4 (Fig. 3a). For samples n-Cu-g-C_3N_4, c-Cu-g-C_3N_4 and s-Cu-g-C_3N_4, Cu element could be detected clearly except the elements C, N and O. In addition, the content of oxygen in c-Cu-g-C_3N_4 and s-Cu-g-C_3N_4 increased obviously, which maybe resulted from the introduction of oxygen-containing groups or the oxidation of copper components. For the XPS C1s spectrum of g-C_3N_4, characteristic peaks locating at 284.6 eV and 288.0 eV were attributed to the sp^2-bonded carbon in C−C and N−C=N bonds respectively [35,36] and the intensity of peak at 288.0 eV is stronger than the peak at 284.6 eV, indicating g-C_3N_4 achieved in our experiment has the standard structure of graphitic carbon nitride. For sample n-Cu-g-C_3N_4, the C1s XPS spectrum has similar contour with g-C_3N_4 but the intensity of peak at 288.0 eV decreased, suggesting the surface structure of g-C_3N_4 in n-Cu-g-C_3N_4 was slightly destroyed. However, the C1s XPS spectra of c-Cu-g-C_3N_4 and s-Cu-g-C_3N_4 exhibited strong peak at 284.6 eV and relative weak peak at 288.0 eV, indicating the damage of surface structure in the two materials. The Cu 2p spectra of n-Cu-g-C_3N_4, c-Cu-g-C_3N_4 and s-Cu-g-C_3N_4 show obvious Cu $2p_{2/3}$ peak at 932.5 eV and Cu $2p_{1/2}$ peak at 952.4 eV, indicating that the main copper component was Cu or Cu_2O [37,38]. For samples c-Cu-g-C_3N_4 and s-Cu-g-C_3N_4, a small peak at about 934.5 eV ascribing to CuO could be deconvolved out, suggesting that there were also Cu (II) species in the two samples [39]. Especially for the sample s-Cu-g-C_3N_4, a weak and broad satellite peak locating at 940−945 eV could be observed, which further confirmed the existence of Cu (II) species in s-Cu-g-C_3N_4 [39]. To clarified the main copper component was Cu or Cu_2O, we carefully analyzed the Cu auger LMM spectra (Fig. 3d). The main peak locating at 571.2 eV indicated that Cu_2O was major existence form of copper in the three samples. A small shoulder peak at 568.0 eV suggested the existence of metal copper in the LMM spectrum of s-Cu-g-C_3N_4 [38,40]. So, we confirmed that oxygen in air oxidized metal copper to cuprous oxide although
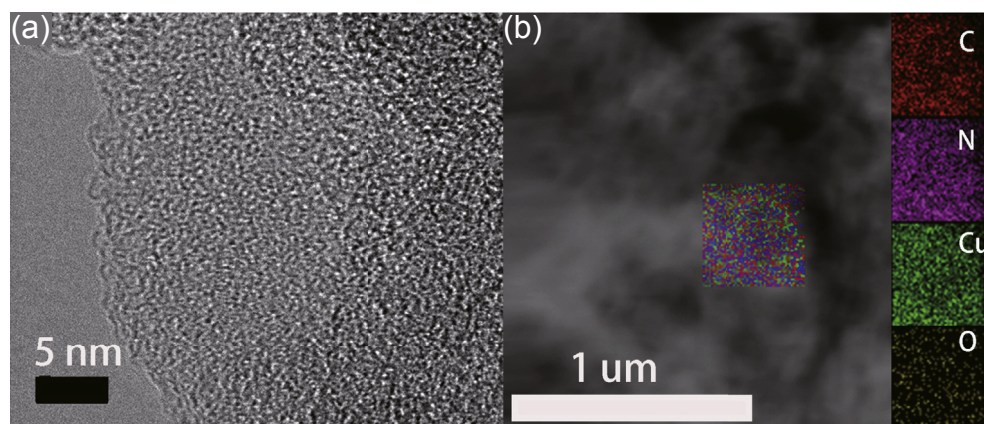

Fig. 2. (a) HRTEM image of n-Cu-g-C_3N_4; (b) EDX mapping image of C, N, Cu and O elements in n-Cu-g-C_3N_4 (the scale bar for element mapping images and STEM image is same).
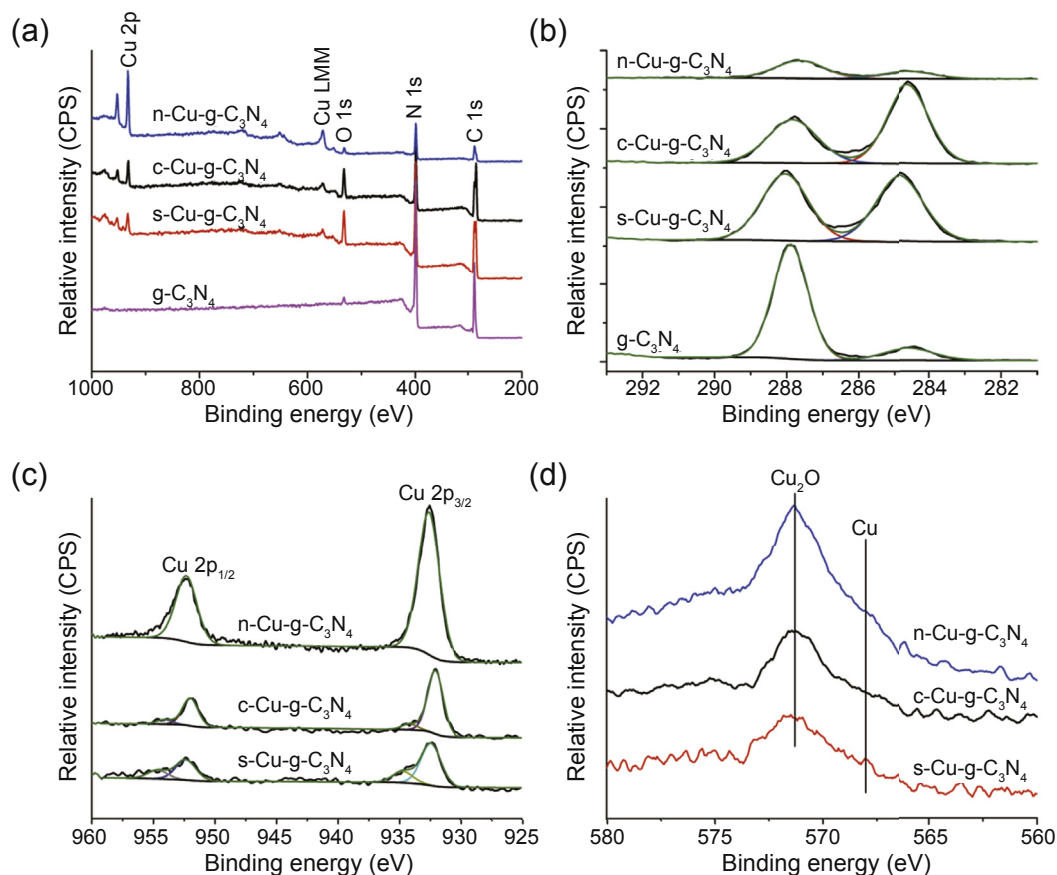
Fig. 3. (a) Full XPS spectrum of g-C$_3$N$_4$, n-Cu-g-C$_3$N$_4$, c-Cu-g-C$_3$N$_4$ and s-Cu-g-C$_3$N$_4$, (b) C1s XPS spectrum of g-C$_3$N$_4$, n-Cu-g-C$_3$N$_4$, c-Cu-g-C$_3$N$_4$ and s-Cu-g-C$_3$N$_4$, (c) Cu 2p XPS spectrum of n-Cu-g-C$_3$N$_4$, c-Cu-g-C$_3$N$_4$ and s-Cu-g-C$_3$N$_4$, (d) Cu auger LMM spectrum of n-Cu-g-C$_3$N$_4$, c-Cu-g-C$_3$N$_4$ and s-Cu-g-C$_3$N$_4$.

the copper component was reduced into metal copper during the synthesis process. In sample s-Cu-g-C$_3$N$_4$, copper component could not be fully oxidized due to the aggregation according the XRD pattern so that three copper species could be detected.

3.2. Catalytic activity

Initially, the N-arylation of pyrazole with iodobenzene as arylating reagent and Cs$_2$CO$_3$ as strong base was selected as model reaction. No coupling product was detected on GC in absent of any catalyst. If 10 mg of n-Cu-g-C$_3$N$_4$ was used as catalyst, the yield of coupling product reached to almost 100%. In control experiments, g-C$_3$N$_4$ and cupric nitrate has no catalytic activity for this coupling reaction, and c-Cu-g-C$_3$N$_4$ and s-Cu-g-C$_3$N$_4$ show poor catalytic performance with 11.4% and 26.5% yields respectively under standard reaction conditions. Combining XPS results and reaction data, the heterogeneous Cu$_2$O components should be catalytic active phase for this reaction and popping process is a key step for achieving catalyst with high catalytic activity. In addition, we evaluated other bases such as NaOH, KOH, Na$_2$CO$_3$ and K$_2$CO$_3$ under same reaction conditions. It was found that NaOH and KOH could achieve moderate yield of product and

the coupling reaction could not be almost conducted with Na$_2$CO$_3$ and K$_2$CO$_3$ as base. This result suggested that the reaction must be promoted by strong base. The higher yield of 100% for coupling product could be achieved if the reaction time was prolonged to 12 h with n-Cu-g-C$_3$N$_4$ as catalyst.

Based on the reaction results and analyses of XPS spectra, XRD profiles and Cu auger LMM spectra, we concluded that Cu$_2$O species were active phased in catalyst for this C–N coupling reaction and then proposed a reasonable catalytic mechanism. Firstly, iodobenzene could be decomposed into phenyl and iodide under the effect of catalyst and heating condition. The phenyl and iodide could be stabilized on the surface of cuprous oxide by adsorption. Secondly, pyrazole ion was generated due to the deprotonation of pyrazole under the effect of strong base, and adsorbed on the surface of cuprous oxide. One HI could be generated from the reaction between the proton and adsorbed iodide on catalyst. Lastly, the adsorbed phenyl and pyrazole ion reacted and generated a final coupling product, and catalyst was restored (Fig. 4).

We also evaluated this catalytic activity for the N-arylation of pyrazole with other iodobenzene derivates and high catalytic performance was achieved. In general, electron-withdrawing group facilitated the coupling reaction because the C–I bond in iodobenzene detrivates become weak under
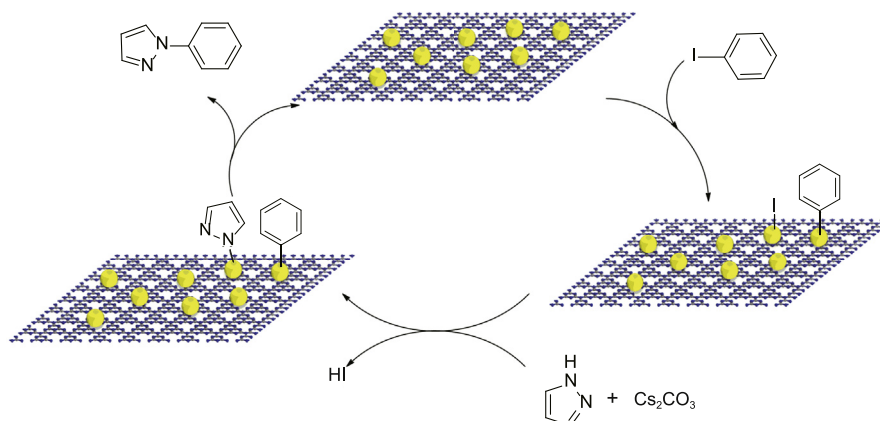
Fig. 4. The proposed catalytic mechanism.

the impact of electron-withdrawing group. In contrast, electron-donating group would make the coupling reaction difficult. In addition, ortho-position substituent group also decreased reactivity due to the steric hindrance effect.

4. Conclusions

By using g-C$_3$N$_4$ and cupric nitrate as precursors, a copper-based catalyst supported on g-C$_3$N$_4$ was developed through a novel popping process which is a key and essential step for the well distribution of copper species and catalytic activity of final catalyst. The catalyst n-Cu-g-C$_3$N$_4$ exhibited excellent catalytic activity in the N-arylation of pyrazole with iodo-benzene derivates. Combining control experiments and characterizations, we demonstrate that Cu$_2$O supported on g-C$_3$N$_4$ was catalytic active species. This work develops a new method to prepare heterogeneous metal (oxide) catalyst supported on g-C$_3$N$_4$ and will expand the application of g-C$_3$N$_4$ in heterogeneous catalytic field.

Conflicts of interest

There are no conflicts to declare.

Acknowledgements

Appendix A. Supplementary data

Supplementary data related to this article can be found at https://doi.org/10.1016/j.gee.2018.08.003.

References

[1] S.E. Allen, R.R. Walvoord, R. Padilla-Salinas, M.C. Kozlowski, Chem. Rev. 113 (2013) 6234–6458.
[2] M.B. Gawande, A. Goswami, F.-X. Felpin, T. Asefa, X. Huang, R. Silva, X. Zou, R. Zboril, R.S. Varma, Chem. Rev. 116 (2016) 3722–3811.
[3] X. Wang, D. He, Y. Huang, Q. Fan, W. Wu, H. Jiang, J. Org. Chem. 83 (2018) 5458–5466.
[4] K.B. Smith, Y. Huang, M.K. Brown, Angew. Chem. Int. Ed. 57 (2018) 6146–6149.
[5] D. Chen, L. Huang, J. Yang, J. Ma, Y. Zheng, Y. Luo, Y. Shen, J. Wu, C. Feng, X. Lv, Tetrahedron Lett. 59 (2018) 2005–2009.
[6] M.-N. Zhao, Z.-J. Zhang, Z.-H. Ren, D.-S. Yang, Z.-H. Guan, Org. Lett. 20 (2018) 3088–3091.
[7] I. Misztalewska-Turkowicz, K.H. Markiewicz, M. Michalak, A.Z. Wilczewska, J. Catal. 362 (2018) 46–54.
[8] M. Rawat, D.S. Rawat, Tetrahedron Lett. 59 (2018) 2341–2346.
[9] K.M. Siyavash, S. Parinaz, K. Melika, A. Mahsa, D. Minoo, M.A. Mostafa, Appl. Organomet. Chem. 32 (2018) e3914.
[10] N.K. Ojha, G.V. Zyryanov, A. Majee, V.N. Charushin, O.N. Chupakhin, S. Santra, Coord. Chem. Rev. 353 (2017) 1–57.
[11] J. Zhang, J. Liu, Q. Peng, X. Wang, Y. Li, Chem. Mater. 18 (2006) 867–871.
[12] C.-H. Kuo, C.-H. Chen, M.H. Huang, Adv. Funct. Mater. 17 (2007) 3773–3780.
[13] H. Zhang, Q. Zhu, Y. Zhang, Y. Wang, L. Zhao, B. Yu, Adv. Funct. Mater. 17 (2007) 2766–2771.
[14] K.X. Yao, X.M. Yin, T.H. Wang, H.C. Zeng, J. Am. Chem. Soc. 132 (2010) 6131–6144.
[15] R.-P. Ye, L. Lin, C.-C. Chen, J.-X. Yang, F. Li, X. Zhang, D.-J. Li, Y.-Y. Qin, Z. Zhou, Y.-G. Yao, ACS Catal. 8 (2018) 3382–3394.
[16] S.T. Hossain, Y. Almesned, K. Zhang, E.T. Zell, D.T. Bernard, S. Balaz, R. Wang, Appl. Surf. Sci. 428 (2018) 598–608.
[17] X. Yang, Q. Meng, G. Ding, Y. Wang, H. Chen, Y.L. Zhu, Y.W. Li, Appl. Catal. A-Gen. 561 (2018) 78–86.
[18] Q. Xin, A. Papavasiliou, N. Boukos, A. Glisenti, J.P.H. Li, Y. Yang, C.J. Philippopoulos, E. Poulakis, F.K. Katsaros, V. Meynen, P. Cool, Appl. Catal. B Environ. 223 (2018) 103–115.
[19] J. Wen, J. Xie, X. Chen, X. Li, Appl. Surf. Sci. 391 (2017) 72–123.
[20] W.-J. Ong, L.-L. Tan, Y.H. Ng, S.-T. Yong, S.-P. Chai, Chem. Rev. 116 (2016) 7159–7329.
[21] S. Bai, X. Wang, C. Hu, M. Xie, J. Jiang, Y. Xiong, Chem. Commun. 50 (2014) 6094–6097.
[22] J. Zhu, P. Xiao, H. Li, S.A.C. Carabineiro, ACS Appl. Mater. Inter. 6 (2014) 16449–16465.
[23] C. Ji, S.-N. Yin, S. Sun, S. Yang, Appl. Surf. Sci. 434 (2018) 1224–1231.
[24] H. Xu, K. Wu, J. Tian, L. Zhu, X. Yao, Green Chem. 20 (2018) 793–797.

[25] G. Shi, L. Yang, Z. Liu, X. Chen, J. Zhou, Y. Yu, Appl. Surf. Sci. 427 (2018) 1165−1173.

[26] A. Mitra, P. Howli, D. Sen, B. Das, K.K. Chattopadhyay, Nanoscale 8 (2016) 19099−19109.

[27] P. Ruiz-Castillo, S.L. Buchwald, Chem. Rev. 116 (2016) 12564−12649.

[28] J.-P. Corbet, G. Mignani, Chem. Rev. 106 (2006) 2651−2710.

[29] J. Bariwal, E. Van der Eycken, Chem. Soc. Rev. 42 (2013) 9283−9303.

[30] P.W. Leonard, D.E. Chavez, P.R. Bowden, E.G. Francois, Propellants, Explos. Pyrotech. 43 (2018) 11−14.

[31] Y. Gao, X. Chen, J. Zhang, H. Asakura, T. Tanaka, K. Teramura, D. Ma, N. Yan, Adv. Mater. 27 (2015) 4688−4694.

[32] H. Wang, S. Jiang, S. Chen, D. Li, X. Zhang, W. Shao, X. Sun, J. Xie, Z. Zhao, Q. Zhang, Y. Tian, Y. Xie, Adv. Mater. 28 (2016) 6940−6945.

[33] L. Lyu, L. Zhang, G. He, H. He, C. Hu, J. Mater. Chem. A 5 (2017) 7153−7164.

[34] H. Li, F. Li, Z. Wang, Y. Jiao, Y. Liu, P. Wang, X. Zhang, X. Qin, Y. Dai, B. Huang, Appl. Catal. B Environ. 229 (2018) 114−120.

[35] L. Muniandy, F. Adam, A.R. Mohamed, A. Iqbal, N.R.A. Rahman, Appl. Surf. Sci. 398 (2017) 43−55.

[36] C. Shaowen, L. Jingxiang, Y. Jiaguo, J. Mietek, Adv. Mater. 27 (2015) 2150−2176.

[37] T. Ghodselahi, M.A. Vesaghi, A. Shafiekhani, A. Baghizadeh, M. Lameii, Appl. Surf. Sci. 255 (2008) 2730−2734.

[38] P. Zhang, T. Wang, H. Zeng, Appl. Surf. Sci. 391 (2017) 404−414.

[39] W. Li, Y. Gao, P. Tang, Y. Xu, D. Ma, J. Energy Chem. 27 (2018) 859−865.

[40] J.-Y. Park, Y.-S. Jung, J. Cho, W.-K. Choi, Appl. Surf. Sci. 252 (2006) 5877−5891.